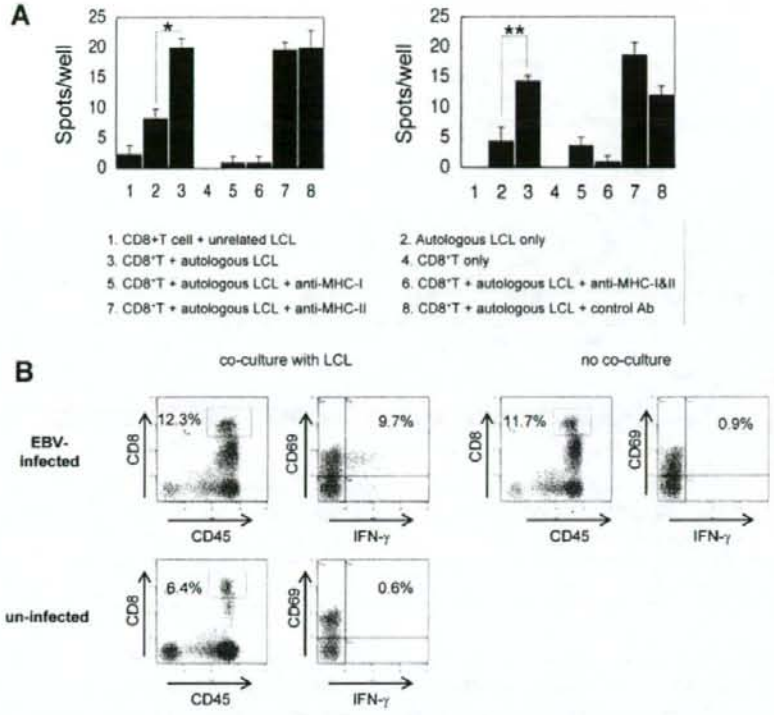

Figure 4. Epstein-Barr virus (EBV)–specific T cell response in humanized NOG (hNOG) mice. *A*, Enzyme-linked immunospot assay for the detection of human T cells producing interferon (IFN)–γ after stimulation with an EBV-positive lymphoblastoid cell line (LCL). $CD8^+$ cells isolated from EBV-infected hNOG mice were cocultured with an autologous LCL, and IFN-γ–secreting cells were counted (3, 5, 6, 7, and 8). To analyze restriction by major histocompatibility complex (MHC), antibody to HLA class I (anti–human HLA-ABC clone W6/32; eBioscience) (5), antibodies to both HLA class I and class II (6), antibody to HLA class II (anti–human HLA-DP,DQ,DR clone CR3/43; Dako) (7), or isotype-matched control antibody (8) were added to the culture. Control experiments included coculture of $CD8^+$ cells with an MHC-mismatched LCL (1), culture of the autologous LCL only (2), and culture of $CD8^+$ cells only (4). Results from 2 infected mice are shown. Five hundred $CD8^+$ cells per well were cultured in the experiment shown on the left, and 250 $CD8^+$ cells per well were cultured in that shown on the right. Spots were counted in triplicate in each of the 8 experimental groups, and the bars represent mean values and SEs. The unpaired Student's *t* test was used for statistical analysis. $^*P < .01$ and $^{**}P < .02$. *B*, Detection of human $CD8^+$ cells that produce IFN-γ in response to stimulation with an EBV-positive LCL by flow cytometry. $CD8^+$ cells were isolated from the spleen of an EBV-infected mouse and cocultured with the autologous LCL. Intracellular IFN-γ was stained and analyzed as described in Methods.

virus died of lymphoproliferative disorder ~5–10 weeks after inoculation. The remaining mice in both of the lots that received lower doses (1×10^1, 1×10^0, and 1×10^{-1} TD_{50}) survived acute infection and appeared normal throughout the observation period of 22 weeks. Although EBV DNA was detected at variable levels in their peripheral blood several weeks after inoculation, it returned to undetectable levels thereafter (figure 1*B*), suggesting that a certain protection mechanism worked to control EBV infection. Importantly, EBV DNA could be still detected in various organs, including spleen, liver, lungs, kidneys, and adrenal glands, at the end of the observation period (22 weeks), indicating that EBV persisted in these mice (table 2). Double staining for EBER and CD20 showed that EBV persisted in B cells (figure 2*G*). Macroscopical examination by autopsy at the end of the observation period did not reveal abnormality in these mice, except for moderate splenomegaly found in a mouse that received 1×10^1 TD_{50}. These results indicate that the outcome of EBV infection in hNOG mice varies with the virus dose; high doses of virus tend to cause fatal lymphoproliferative disorder, whereas lower doses induce apparently asymptomatic persistent infection.

EBV-specific T cell response in hNOG mice. Flow cytometry analysis demonstrated a dramatic increase in the percentage of $CD3^+$ T cells among the human $CD45^+$ leukocytes after infection with EBV. This increase in T cells was accompanied by an increase in the percentage of $CD8^+$ cells among human $CD3^+$ T cells. These changes were seen in virtually all infected mice, and the results from 3 mice are shown in figure 3*A*. The slow increase in the percentage of $CD3^+$ cells in the uninfected mouse represents the process of humanization (i.e., the development of hu-

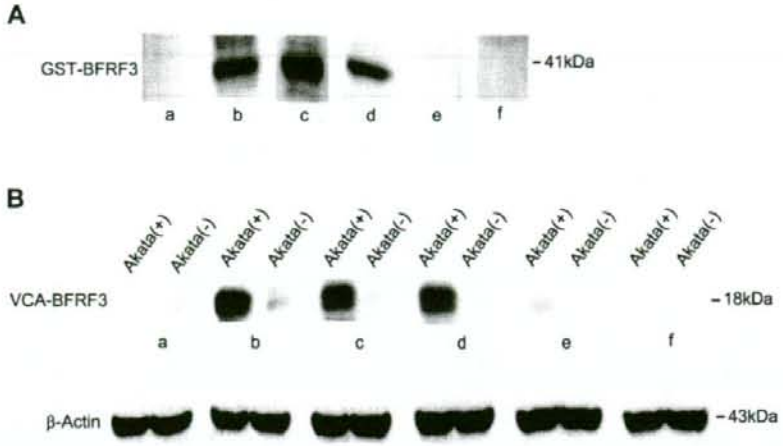

Figure 5. Demonstration of IgM antibody to the Epstein-Barr virus (EBV) BFRF3 protein in the serum of humanized NOG (hNOG) mice. *A*, Immunoblot with the glutathione *s*-transferase (GST)–BFRF3 fusion protein. Purified GST-BFRF3 fusion protein was examined with serum from an EBV-uninfected person *(a)*, an EBV-infected person *(b)*, EBV-infected hNOG mice (*c* and *d*), and an uninfected hNOG mice (*e* and *f*). *B*, Immunoblot with the lysate of EBV-producing Akata cells. Lysate of anti-IgG–treated Akata cells, labeled Akata(+), and of EBV-negative Akata cells, labeled Akata(−), was examined using serum from an EBV-uninfected person *(a)*, an EBV-infected person *(b)*, EBV-infected hNOG mice (*c* and *d*), and uninfected hNOG mice (*e* and *f*).

man T cells). This increase in $CD8^+$ cells were even more conspicuous when their definite number was counted (figure 3*B*). When hNOG mice were inoculated with serially diluted virus samples, a striking dose response was evident; mice inoculated with higher doses exhibited a more profound increase in $CD8^+$ cells at earlier time points (figure 3*C*). Further flow cytometry analyses showed that $CD45RO^+$ memory T cells, compared with $CD45RA^+$ T cells, increased in infected hNOG mice (figure 3*D*). Expression of a T cell activation marker, HLA-DR, was observed mainly in $CD8^+$ cells rather than in $CD4^+$ cells (figure 3*D*).

To demonstrate that these $CD8^+$ T cells were directed against EBV-infected cells, we examined IFN-γ secretion after stimulation with EBV-transformed cells. For this purpose, we first established an LCL using B cells isolated from the same cord blood that was used to isolate HSCs for transplantation. $CD8^+$ T cells, isolated from the peripheral blood of EBV-infected hNOG mice, were incubated with this autologous LCL, and cells secreting IFN-γ were detected by ELISPOT assay. For all 3 EBV-infected hNOG mice (which had been infected at 1×10^3 TD_{50}) thus examined, a significant number of spots were recognized in the wells in which $CD8^+$ T cells were mixed with the autologous LCL, whereas those cells incubated with unrelated LCL had many fewer spots (data from 2 mice are shown in figure 4*A*). $CD8^+$ T cells isolated from uninfected hNOG mice did not give a significant number of spots (data not shown). Release of IFN-γ was blocked by antibody specific to human major histocompatibility complex (MHC) class I but not by that specific to human MHC class II (figure 4*A*). These results clearly show that a T cell response restricted by human MHC class I was mounted against EBV-infected cells. In addition, in 5 of the 6 EBV-infected hNOG mice examined (infected at 1×10^3 TD_{50}), flow cytometry also demonstrated production of IFN-γ by $CD8^+$ T cells isolated from the spleen and stimulated with an autologous LCL (figure 4*B*).

EBV-specific antibody response in hNOG mice. Serum samples from 30 EBV-infected hNOG mice were examined by Western blotting for IgM antibodies reactive with a bacterially expressed GST-BFRF3 fusion protein. The BFRF3 protein is a major component of the virus capsid antigen of EBV [26]. The results are shown in figure 5*A* and indicated that four serum samples (from mice infected at 1×10^1 or 1×10^3 TD_{50}) contained IgM antibody reactive with it. These serum samples reacted also with the 18-kDa BFRF3-encoded protein in the lysate of Akata cells stimulated with IgG antibody to activate virus production (figure 5*B*). Similar experiments with human IgG–specific secondary antibody did not show a positive reaction with either GST-BFRF or $p18^{BFRF3}$. Six serum samples collected from uninfected hNOG mice reacted with neither the 18-kDa protein nor GST-BFRF3 (figure 5 and data not shown). These results indicate that hNOG mice have the ability to mount an IgM response to EBV.

DISCUSSION

The lymphoproliferative disease induced in hNOG mice is remarkably similar to the human lymphoproliferative disorder seen in immunocompromised hosts [27] with respect to histology, surface phenotype, and the type of EBV gene expression

(latency III). Reproduction of latency III in the present study makes for an interesting contrast with the previous model using NOD/*scid* mice, which exhibited the latency II pattern [10].

EBV infection in lower doses resulted in a transient increase in EBV DNA load in the peripheral blood, followed by apparently asymptomatic infection that persisted for at least 22 weeks. This type of asymptomatic EBV infection has not been described in nonprimate models of EBV infection and may be regarded as a model of human EBV latency. To compare this condition in NOG mice with EBV latency in humans precisely, we need to further investigate the nature of host cells (i.e., whether they are memory B cells), the pattern of EBV gene expression in them, and the involvement of anti-EBV immune responses in its maintenance.

In hNOG mice, human T cells develop in thymus tissue, in which epithelial cells are of murine origin [16]. It is therefore interesting that they could mount a T cell response restricted by human MHC class I. Although this suggests that positive selection of human T cells occurred in hNOG mice, the mechanism of T cell education remains unclear. Alloantigen-specific and human MHC class I–restricted T cell cytotoxicity has been reported in hNOG mice [15, 16]. An EBV-induced T cell response was evident in mice that received high doses of virus and developed lymphoproliferative disorder, suggesting that the T cell response in hNOG mice was not sufficient to control EBV-induced lymphoproliferation when they were infected at high doses. That only a minor fraction of $CD8^+$ T cells appeared to be EBV specific, as evidenced by ELISPOT assay and flow cytometry, may explain this result, at least partially. A humoral immune response to EBV has not been documented in previous mouse models of EBV infection, and therefore the NOG mouse may provide a valuable tool to analyze the mechanism and the protective roles of antibody response in EBV infection. We have to date clearly identified only IgM antibody to the 18-kDa component of virus capsid antigen in a minor fraction (4/30) of infected mice. We are currently attempting to improve sensitivity and to see whether hNOG mice can mount a more efficient and divergent antibody response to the virus, possibly including the production of IgG antibodies. Because both the T cell–mediated and the humoral immune response are elicited in hNOG mice, they may be useful in the evaluation of candidate EBV vaccines.

Very recently, humanized mice based on other immunodeficient mouse strains were prepared, and EBV was used as a typical pathogen to analyze their immune functions. Traggiai et al. [12] infected humanized $Rag2^{-/-}$IL-$2R\gamma^{-/-}$ mice with EBV and documented an in vitro proliferative response by $CD8^+$ T cells to an autologous LCL. Melkus et al. [11], on the other hand, humanized NOD/*scid* mice by transplanting human fetal liver, thymus, and HSCs and succeeded in inducing an EBV-specific T cell immune response as well as an innate immune response to toxic shock syndrome toxin 1. These 2 studies were performed mainly using immunological standpoints and did not provide detailed data from virological investigations. An advantage of the NOG mouse model described here is that it does not require a fine surgical procedure using human fetal tissue; therefore, NOG mice can be easily provided in large quantities.

In immunocompromised humans, failure of immunosurveillance may lead to the development of lymphoproliferative disorder. We expect that the NOG mouse model can be used to analyze the exact relationship between immunodeficiency and the development of lymphoproliferative disorder. Immune responses in the hNOG mouse can be modulated by immunosuppressive drugs (such as cyclosporine A) or HIV, and the development of lymphoproliferative disorder can be analyzed with special reference to the nature and level of immunodeficiency. This kind of study, which has not been possible with conventional *scid* mice, may reveal an exact condition in which lymphoproliferative disorder develops and may thereby aid the development of a specified immunosuppressive procedure that evades this condition and precludes the risk of lymphoproliferative disorder.

In summary, the NOG mouse is able to recapitulate various essential elements of human EBV infection and is therefore, to our knowledge, the most comprehensive small-animal model of EBV infection described to date. It should be a valuable tool for the study of the pathogenesis, prevention, and treatment of EBV infection.

Acknowledgments

We thank Satoshi Itakura, Fuyuko Kawano, Eri Yamada, Miki Mizukami, and Ken Watanabe for technical assistance. We thank Shizuko Minegishi for advice on flow cytometry, Atsushi Komano for advise on the enzyme-linked immunospot assay, Ayako Demachi-Okamura and Kiyotaka Kuzushima for advice on detection of Epstein-Barr virus–specific T cells, and Shosuke Imai for helpful discussions. We thank the Tokyo Cord Blood Bank for supplying cord blood.

References

1. Rickinson AB, Kieff E. Epstein-Barr virus. In: Knipe DM, Howley PM, eds. Fields virology. Philadelphia: Lippincott Williams & Wilkins, **2001**: 2575–628.
2. Kieff E, Rickinson AB. Epstein-Barr virus and its replication. In: Knipe DM, Howley PM, eds. Fields virology. 4th ed. Philadelphia: Lippincot Williams & Wilkins, **2001**:2511–74.
3. Young LS, Finerty S, Brooks L, Scullion F, Rickinson AB, Morgan AJ. Epstein-Barr virus gene expression in malignant lymphomas induced by experimental virus infection of cottontop tamarins. J Virol **1989**; 63: 1967–74.
4. Miller G, Shope T, Coope D, et al. Lymphoma in cotton-top marmosets after inoculation with Epstein-Barr virus: tumor incidence, histologic spectrum antibody responses, demonstration of viral DNA, and characterization of viruses. J Exp Med **1977**; 145:948–67.
5. Cho Y, Ramer J, Rivailler P, et al. An Epstein-Barr-related herpesvirus from marmoset lymphomas. Proc Natl Acad Sci USA **2001**; 98:1224–9.
6. Moghaddam A, Rosenzweig M, Lee-Parritz D, Annis B, Johnson RP, Wang F. An animal model for acute and persistent Epstein-Barr virus infection. Science **1997**; 276:2030–3.
7. Mosier DE, Gulizia RJ, Baird SM, Wilson DB. Transfer of a functional human immune system to mice with severe combined immunodeficiency. Nature **1988**; 335:256–9.

8. Okano M, Taguchi Y, Nakamine H, et al. Characterization of Epstein-Barr virus-induced lymphoproliferation derived from human peripheral blood mononuclear cells transferred to severe combined immunodeficient mice. Am J Pathol **1990**; 137:517–22.
9. Rowe M, Young LS, Crocker J, Stokes H, Henderson S, Rickinson AB. Epstein-Barr virus (EBV)-associated lymphoproliferative disease in the SCID mouse model: implications for the pathogenesis of EBV-positive lymphomas in man. J Exp Med **1991**; 173:147–58.
10. Islas-Ohlmayer M, Padgett-Thomas A, Domiati-Saad R, et al. Experimental infection of NOD/SCID mice reconstituted with human CD34+ cells with Epstein-Barr virus. J Virol **2004**; 78:13891–900.
11. Melkus MW, Estes JD, Padgett-Thomas A, et al. Humanized mice mount specific adaptive and innate immune responses to EBV and TSST-1. Nat Med **2006**; 12:1316–22.
12. Traggiai E, Chicha L, Mazzucchelli L, et al. Development of a human adaptive immune system in cord blood cell-transplanted mice. Science **2004**; 304:104–7.
13. Hiramatsu H, Nishikomori R, Heike T, et al. Complete reconstitution of human lymphocytes from cord blood CD34+ cells using the NOD/SCID/γ_c^{null} mice model. Blood **2003**; 102:873–80.
14. Ito M, Hiramatsu H, Kobayashi K, et al. NOD/SCID/γ_c^{null} mouse: an excellent recipient mouse model for engraftment of human cells. Blood **2002**; 100:3175–82.
15. Yahata T, Ando K, Nakamura Y, et al. Functional human T lymphocyte development from cord blood CD34+ cells in nonobese diabetic/Shi-scid, IL-2 receptor gamma null mice. J Immunol **2002**; 169:204–9.
16. Ishikawa F, Yasukawa M, Lyons B, et al. Development of functional human blood and immune systems in NOD/SCID/IL2 receptor γ chain^{null} mice. Blood **2005**; 106:1565–73.
17. Miyazato P, Yasunaga J, Taniguchi Y, Koyanagi Y, Mitsuya H, Matsuoka M. De novo human T-cell leukemia virus type 1 infection of human lymphocytes in NOD-SCID, common gamma-chain knockout mice. J Virol **2006**; 80:10683–91.
18. Watanabe S, Terashima K, Ohta S, et al. Hematopoietic stem cell-engrafted NOD/SCID/IL2Rgamma null mice develop human lymphoid systems and induce long-lasting HIV-1 infection with specific humoral immune responses. Blood **2007**; 109:212–8.
19. Dewan MZ, Terashima K, Taruishi M, et al. Rapid tumor formation of human T-cell leukemia virus type 1-infected cell lines in novel NOD-SCID/gammac^{null} mice: suppression by an inhibitor against NF-kappaB. J Virol **2003**; 77:5286–94.
20. Watanabe S, Ohta S, Yajima M, et al. Humanized NOD/SCID/IL2Rγ^{null} mice transplanted with hematopoietic stem cells under nonmyeloablative conditions show prolonged life spans and allow detailed analysis of human immunodeficiency virus type 1 pathogenesis. J Virol **2007**; 81: 13259–64.
21. Takada K, Ono Y. Synchronous and sequential activation of latently infected Epstein-Barr virus genomes. J Virol **1989**; 63:445–9.
22. Condit RC. Principles of virology. In: Knipe DM, Howley PM, eds. Fields virology. Philadelphia: Lippincott Williams & Wilkins, **2001**:19–51.
23. Kimura H, Morita M, Yabuta Y, et al. Quantitative analysis of Epstein-Barr virus load by using a real-time PCR assay. J Clin Microbiol **1999**; 37:132–6.
24. Nakamura H, Iwakiri D, Ono Y, Fujiwara S. Epstein-Barr-virus-infected human T-cell line with a unique pattern of viral-gene expression. Int J Cancer **1998**; 76:587–94.
25. Kuzushima K, Hoshino Y, Fujii K, et al. Rapid determination of Epstein-Barr virus-specific CD8$^+$ T-cell frequencies by flow cytometry. Blood **1999**; 94:3094–100.
26. van Grunsven WM, Nabbe A, Middeldorp JM. Identification and molecular characterization of two diagnostically relevant marker proteins of the Epstein-Barr virus capsid antigen complex. J Med Virol **1993**; 40: 161–9.
27. Rezk SA, Weiss LM. Epstein-Barr virus-associated lymphoproliferative disorders. Hum Pathol **2007**; 38:1293–304.

ELSEVIER

INSTITUT PASTEUR

Microbes and Infection 10 (2008) 748–756

www.elsevier.com/locate/micinf

Original article

Induction of apoptosis in Epstein-Barr virus-infected B-lymphocytes by the NF-κB inhibitor DHMEQ

Ariko Miyake [a,1], Md. Zahidunnabi Dewan [b,c,1], Takaomi Ishida [a], Mariko Watanabe [d], Mitsuo Honda [c], Tetsutaro Sata [e], Naoki Yamamoto [b,c,**], Kazuo Umezawa [f], Toshiki Watanabe [a,***], Ryouichi Horie [d,*]

[a] *Laboratory of Tumor Cell Biology, Department of Medical Genome Sciences, Graduate School of Frontier Sciences, University of Tokyo, 4-6-1 Shirokanedai, Minato-ku, Tokyo 108-8639, Japan*

[b] *Department of Molecular Virology, Bio-Response, Graduate School, Tokyo Medical and Dental University, 1-5-45 Yushima, Bunkyo-ku, Tokyo 113-8519, Japan*

[c] *AIDS Research Center, National Institute of Infectious Diseases, 1-23-1 Toyama, Shinjuku-ku, Tokyo 162-8640, Japan*

[d] *Department of Hematology, School of Medicine, Kitasato University, 1-15-1 Sagamihara, Kanagawa 228-8555, Japan*

[e] *Department of Pathology, National Institute of Infectious Diseases, 1-23-1 Toyama, Shinjuku-ku, Tokyo 162-8640, Japan*

[f] *Department of Applied Chemistry, Faculty of Science and Technology, Keio University, 3-14-1 Hiyoshi, Kohoku-ku, Yokohama, Kanagawa 223-0061, Japan*

Received 19 January 2008; accepted 9 April 2008
Available online 13 April 2008

Abstract

Epstein–Barr virus (EBV) causes EBV-associated lymphoproliferative diseases in patients with profound immune suppression. Most of these diseases are life-threatening and the prognosis of AIDS-associated lymphomas is extremely unfavorable. Polyclonal expansion of virus infected B-cell predisposes them to transformation. We investigated the possibility of nuclear factor kappa B (NF-κB) inhibition by dehydroxymethylepoxyquinomicin (DHMEQ) for the treatment and prevention of EBV-associated lymphoproliferative diseases. We examined the effect of DHMEQ on apoptosis induction in four EBV-transformed lymphoblastoid cell lines as well as peripheral blood mononuclear cells infected with EBV under immunosuppressed condition. DHMEQ inhibits NF-κB activation in EBV-transformed lymphoblastoid cell lines and induces apoptosis by activation of mitochondrial and membranous pathways. Using an *in vivo* NOD/SCIDγc mouse model, we showed that DHMEQ has a potent inhibitory effect on the growth of lymphoblastoid cells. In addition, DHMEQ selectively purges EBV-infected cells expressing latent membrane protein (LMP) 1 from peripheral blood mononuclear cells and inhibits the outgrowth of lymphoblastoid cells. These results suggest that NF-κB is a molecular target for the treatment and prevention of EBV-associated lymphoproliferative diseases. As a potent NF-κB inhibitor, DHMEQ is a potential compound for applying this strategy in clinical medicine.

Keywords: Epstein–Barr virus infections; NF-κB; DHMEQ

1. Introduction

Epstein–Barr virus (EBV) is a member of the γ-herpesvirus family that infects more than 90% of the world population and initially establishes latency III infection in B lymphocytes [1]. Latency III infection is characterized by the expression of the entire array of EBV latency genes, including EBV nuclear proteins (EBNA1, -2, -3A, -3B, -3C, and -LP), integral latent membrane proteins (LMP1, -2A, and -2B), the BamA

* Corresponding author. Tel.: +81 42 778 8111; fax: +81 42 778 8441.
** Tel.: +81 3 5803 5178; fax: +81 3 5803 0124.
*** Tel.: +81 3 5449 5298; fax: +81 3 5449 5418.
E-mail addresses: yamamoto.mmb@tmd.ac.jp (N. Yamamoto), tnabe@ims.u-tokyo.ac.jp (T. Watanabe), rhorie@med.kitasato-u.ac.jp (R. Horie).
[1] These authors contributed equally to this work.

1286-4579/$ - see front matter © 2008 Elsevier Masson SAS. All rights reserved.
doi:10.1016/j.micinf.2008.04.002

rightward transcripts (BARTs), and small RNAs (EBERs). Immune response mediated by T-lymphocytes eliminates most latency III-infected cells; however, resting memory B lymphocytes provide a reservoir for latent virus. T-lymphocyte immunity to latency III-infected B lymphocytes persists for life and protects reactivation of latent virus from a reservoir [2].

However, in the absence of an effective immune response, reactivation of latent virus from a reservoir occurs and causes EBV-associated lymphoproliferative diseases. EBV-associated lymphoproliferative diseases occur with primary infection after transplantation or reactivation of latent virus as a consequence of immune suppression for organ transplantation and autoimmune diseases or acquired immune deficiency syndrome (AIDS) [3–6]. EBV-associated lymphoproliferative diseases are associated in the majority of cases with latency type III phenotype. The prognosis of EBV-associated lymphoproliferative diseases is variable; however, most of these are life-threatening and the prognosis of AIDS-associated lymphomas is extremely unfavorable, although introduction of highly active anti-retroviral treatment (HAART) decreased the incidence, increased the effectiveness of chemotherapy, and improved survival [5]. EBV infection of B-lymphocytes *in vitro* also results in latency III infection and sustained cell proliferation as lymphoblastoid cell lines (LCLs).

Activation of nuclear factor kappa B (NF-κB) has been connected with resistance against apoptosis and tumorigenesis [7]. Despite the diversity in clinical manifestations of EBV-associated lymphoproliferative diseases, strong and constitutive NF-κB activity is reported to be a common characteristic of this disease entity. LMP1 mimics signaling from tumor necrosis factor (TNF) receptor family members by association with tumor necrosis factor receptor-associated factors (TRAFs) and activates the IKK (IκB kinase)–NF-κB pathway [8].

NF-κB represents five cellular proteins: c-Rel, RelA (p65), RelB, NF-κB1 (p50 and its precursor p105), and NF-κB2 (p52 and its precursor p100). The IκB inhibitory proteins consist of IκBα, IκBβ, IκBε, IκBγ, and Bcl-3. NF-κB forms homo- or heterodimers and exists as an inactive complex with IκB regulatory proteins in the cytoplasm. Various signaling pathways converge into IKK-mediated degradation of IκB proteins and subsequent release of uncomplexed NF-κB, which then migrates into the nucleus and activates the transcription of target genes [9].

Dehydroxymethylepoxyquinomicin (DHMEQ) is a new NF-κB inhibitor that is a 5-dehydroxymethyl derivative of the novel compound epoxyquinomicin C that has a 4-hydroxy-5,6-epoxycyclohexenone structure like panepoxydone. Panepoxydone had been found to inhibit TNF-α-induced activation of NF-κB [10]. We have shown that DHMEQ inhibits NF-κB at the level of nuclear translocation [11].

In this study, to investigate the possibility of NF-κB inhibition by DHMEQ as a strategy for the treatment and prevention of EBV-associated lymphoproliferative diseases, we investigated the effect of DHMEQ on apoptosis induction in four EBV-transformed LCLs as well as peripheral blood mononuclear cells (PBMC) in the early phase of EBV infection, and further examined the molecular mechanism of DHMEQ-induced apoptosis.

2. Materials and methods

2.1. Cells

B95.8 EBV-transformed LCLs were established by infection of lymphocytes from four healthy donors with culture supernatants of the virus producer B95.8 line as described previously [12], and are indicated in the text by the first two letters of the name of each donor. In all experiments to test the effects of DHMEQ treatment, LCLs were maintained in RPMI 1640 medium supplemented with 10% fetal bovine serum (FBS).

2.2. Chemicals

DHMEQ is an NF-κB inhibitor that blocks nuclear translocation of NF-κB [11]. DHMEQ was dissolved with dimethylsulfoxide (DMSO). DHMEQ or DMSO was used for experiments at indicated concentrations. Bisbenzimide H 33342 fluorochrome (Hoechst 33342) was purchased from Calbiochem (Bad Soden, Germany).

2.3. Electrophoretic mobility shift analysis

Electrophoretic mobility shift analysis (EMSA) was carried out according to the methods described previously [13]. For detecting NF-κB binding, a double-stranded oligonucleotide containing the κB site of the promoter for the mouse H-2Kb class I major histocompatibility antigen gene was used as a probe [14]. The nucleotide sequence is 5′-GAT CCG GCT GGG AAT CCC CGC TGG GAA TCC CCA TCT A-3′. For control EMSA, a double-strand oligonucleotide containing Oct-1 consensus sequence (Promega, Madison, WI, USA) was used as a probe. Antibodies used for supershift assays were as follows: NF-κB p50 (C-19) goat polyclonal antibody, rabbit polyclonal antibody for NF-κB p65 (C-20) and RelB (C-19), and mouse monoclonal antibody for c-Rel (B-6) and NF-κB p52 (C-5) (all from Santa Cruz Biotechnology Inc., Santa Cruz, CA). A mouse IgG antibody (Sigma, St. Louis, MO) served as a control.

2.4. Cell viability assay

The effects of DHMEQ on cell viability were assayed by color reaction with a tetrazolium salt, WST-8(4-[3-(2-methoxy-4-nitrophenyl)-2-[4-nitrophenyl]-2*H*-5-tetrazolio]-1,3-benzene disulfonate sodium salt) (Cell Counting Kit-8; Dojindo Laboratories, Kumamoto, Japan). After incubation with DHMEQ or DMSO at the indicated concentrations and time points, cells were treated with Cell Counting Kit-8 according to the manufacturer's recommendations and the results were measured by a microplate reader (Bio-Rad, Richmond, CA) at a test wavelength of 450 nm and reference wavelength of 630 nm.

2.5. Analysis of apoptosis and caspase activities

To quantify apoptosis, cells were labeled with fluorescein isothiocyanate (FITC)-conjugated Annexin V (BD Biosciences, Palo Alto, CA), then subjected to flow cytometric analysis. For analysis of nuclear DNA fragmentation, the terminal deoxynucleotidyl transferase (TdT)-mediated dUTP nick end-labeling (TUNEL) assay was done according to the manufacturer's recommendations (DeadEnd Fluorometric TUNEL Systems; Promega). Cells were analyzed using a FACS Calibur flow cytometer (BD Biociences) and fluorescence microscopy. Activities of caspase-3, -8, and -9 were determined by using green fluorochrome-labeled inhibitors of caspases (FLICA)-3, -8, and -9 (FLICA Apoptosis Detection Kit; Immunochemistry Technologies, Bloomington, MN). Cells from LCLs were treated with 10 μg/ml of DHMEQ (+) or with DMSO alone (−) for 8 h and fixed on slides; active caspases were detected by FLICA-3, -8, and -9. For detection of nuclear DNA, cells were stained with Hoechst 33342 and photographed through a UV filter and an Olympus BX50F microscope (Olympus, Tokyo, Japan).

2.6. In vivo effects of DHMEQ on NOG mice inoculated with LCLs

NOG mice were purchased from the Central Institute for Experimental Animals (Kawasaki, Japan). The Ethical Review

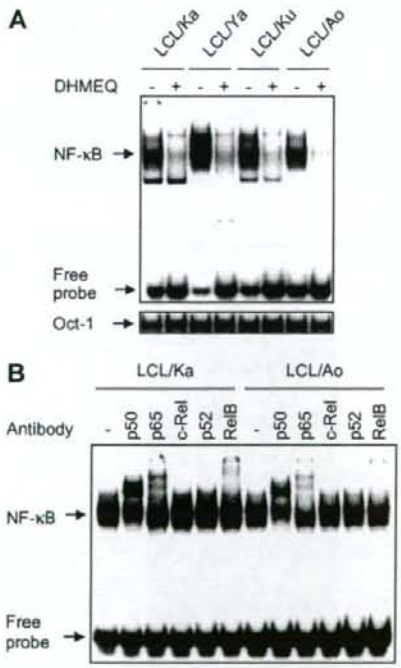

Fig. 1. Inhibition of constitutive NF-κB binding activity in LCLs by DHMEQ. (A) Inhibition of constitutive NF-κB activity in LCLs. LCLs were treated with 10 μg/ml of DHMEQ (+) or with DMSO alone (−) for 3 h. Nuclear extracts (2.5 μg) were examined for NF-κB binding activity by electrophoretic mobility shift analysis (EMSA) with a radiolabeled NF-κB-specific probe. Binding of Oct-1 served as a control. (B) Subcomponents of constitutive NF-κB activity in LCLs. Nuclear extracts (1 μg) of cells without DHMEQ treatment were subjected to supershift analysis with antibodies specific for NF-κB p50, p65, c-Rel, p52, and RelB or without antibody (−). The experiment using isotype matched IgG control showed the same result (data not shown). The position of shifted bands corresponding to NF-κB and free probes are indicated on the left.

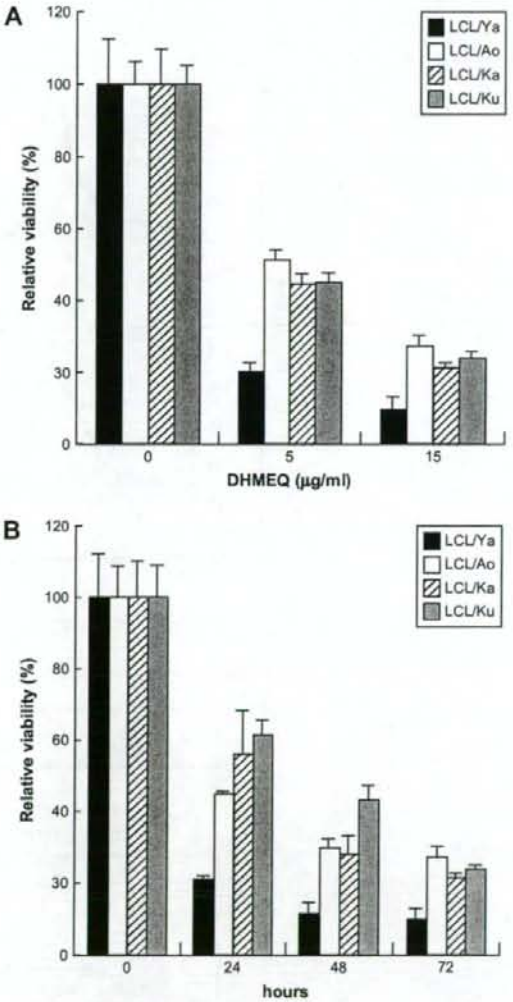

Fig. 2. DHMEQ inhibits proliferation of LCLs. The viability of the cells was determined by WST-8 assay and the relative levels compared with those of DMSO-treated cells are presented. Data represent the mean and standard deviation of triplicate experiments. (A) Results of dose–response experiments. LCLs were treated with 0, 5, or 10 μg/ml of DHMEQ for 72 h. ALL LCLs treated with 0, 5, or 10 μg/ml of DHMEQ showed statistical significance compared to DMSO-treated controls. (B) Results of time–response experiments. LCLs were treated with 10 μg/ml of DHMEQ for 24, 48, and 72 h. ALL LCLs treated for 24, 48, and 72 h except for LCL/Ku at the point of 24 h showed statistical significance compared to DMSO-treated controls.

Committee of the National Institute of Infectious Diseases approved the experimental protocol. 1×10^6 LCL cells were inoculated subcutaneously into the post-auricular region of NOG mice. DHMEQ was administered three times a week for 1 month into the post-auricular region of mice at a dose of 12 mg/kg, beginning on day 5 when tumors were palpable. The control mice were injected RPMI-1640 as was performed in our recent published papers [15,16]. Mice were killed 1 month after inoculation.

2.7. Immunohistochemistry

Cells were immunostained with antibodies and fluorescence signals were detected using confocal microscopy. Cytospin samples were prepared using 5×10^5 cells and cells were first washed three times with phosphate-buffered saline (PBS). Cells were then fixed with 100% cold acetone for 10 min at room temperature and washed three times in PBS. Samples were incubated with primary antibody at the concentration

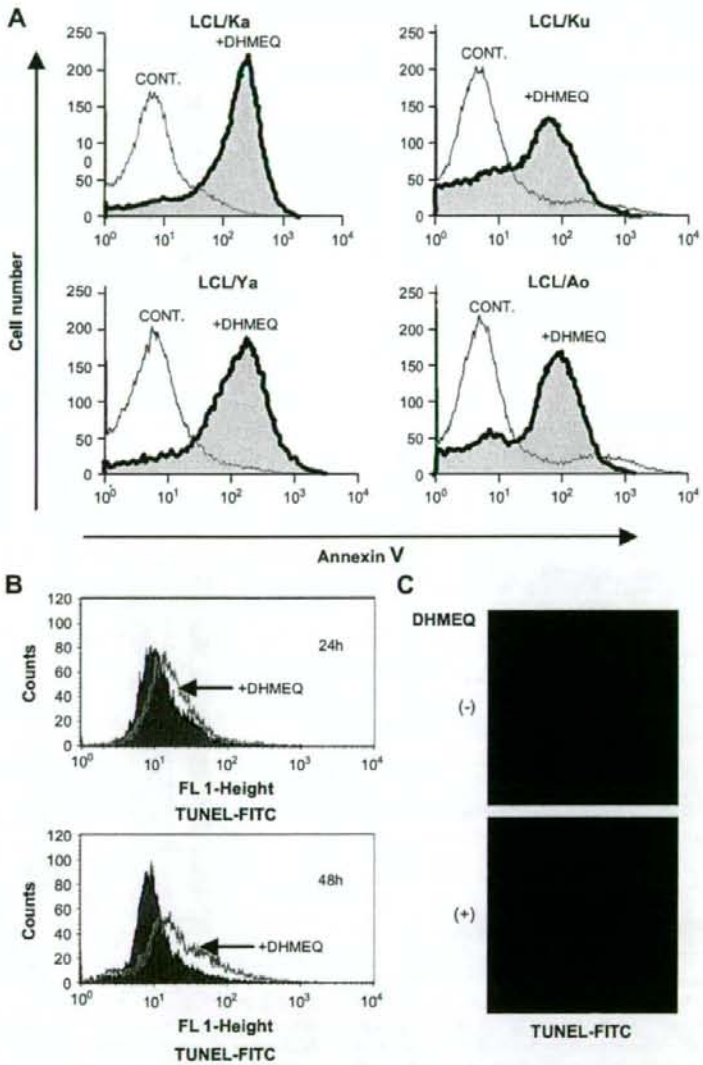

Fig. 3. DHMEQ induces apoptosis in LCLs. (A) Annexin V reactivity in LCLs after DHMEQ treatment. LCLs were treated with (filled curve) or without (open curve) 10 μg/ml of DHMEQ for 48 h, and the binding of FITC-conjugated Annexin V was analyzed by flow cytometry. (B) DNA fragmentation in LCL cells after DHMEQ treatment. DNA fragmentation in LCL cells was detected by TUNEL assay with flow cytometry. Representative flow cytometric profiles are shown for cells treated with 10 μg/ml of DHMEQ (open curve) or with DMSO alone (filled curve) for 24 h (upper panel) or 48 h (lower panel). (C) LCL cells were treated with 10 μg/ml of DHMEQ (+) or with DMSO alone (−) for 48 h, fixed on slides, and processed for TUNEL assay. A filter that selectively detects fluorescein isothiocyanate (FITC)-TUNEL fluorescence was used for the microscopic observation.

of 5 μg/ml at 4 °C overnight and washed with PBS three times. After incubation with fluorescence-labeled secondary antibody for 30 min at 37 °C, samples were washed three times in PBS and covered with a Perma Fluoro antifade reagent (Therme Shandon Co., Pittsburgh, PA). Fluorescence signals were detected using confocal microscopy (Radiance 2000) (Bio-Rad Laboratories. Antibodies used were as follows: anti-Epstein–Barr virus LMP clones CS, 1-4 mouse monoclonal antibody (Dako, Kyoto, Japan), and anti-p65 (c-20) goat polyclonal antibody (Santa Cruz Biotechnology Inc.

2.8. Real-time quantitative PCR

The expression level of anti-apoptotic genes was quantified by real-time reverse transcription–polymerase chain reaction (RT–PCR). Total RNA was extracted from the cells by ISOGEN reagent (Nippon Gene Co., Toyama, Japan) and treated according to the manufacturer's instructions. cDNA was synthesized using oligo dT and random primers synthesized with a PrimeScript RT reagent kit (Takara Bio Inc., Shiga, Japan). Amplification was performed with SYBR premix Ex Taq (Takara Bio Inc.) and the primer sets for c-IAP1, Bfl-1, BCL-XL, and c-FLIP (Takara Bio Inc.). The viral DNA load in EBV-infected PBMC was determined by real-time PCR with slight modifications of a previously described method [17]. DNA samples were extracted from the cells with a DNeasy tissue kit (Qiagen, Hilden, Germany). Amplification with SYBR premix Ex Taq (Takara Bio Inc.) and primers for BALF5 gene encoding the viral DNA polymerase (5′-CGG AAG CCC TCT GGA CTT C-3′ and 5′-CCC TGT TTA TCC GAT GGA ATG-3′) was performed using the Thermal Cycler Dice Real Time System (Takara Bio Inc.) and analyzed using the manufacturer's software.

2.9. Statistical analysis

Differences between mean values were assessed by *t*-test. A *P*-value of <0.05 was considered to be statistically significant.

3. Results

3.1. DHMEQ efficiently blocks constitutive NF-κB activity in LCLs

We first examined the effects of DHMEQ against constitutive NF-κB activity in established LCLs. Treatment with DHMEQ at a concentration of 10 μg/ml abrogated constitutive NF-κB binding activity in these cell lines (Fig. 1A). Components of NF-κB that are constitutively activated in LCLs were analyzed by

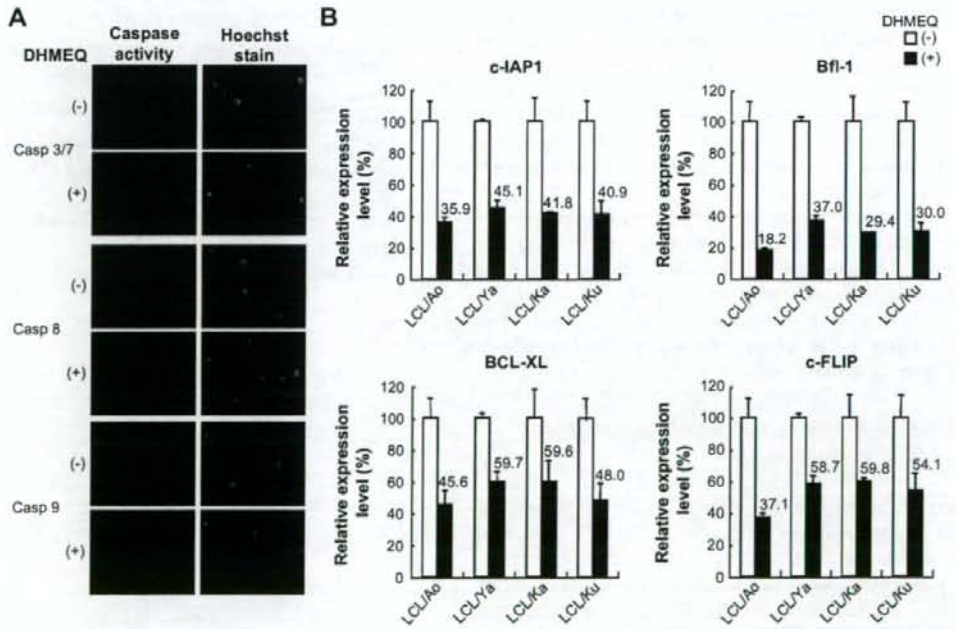

Fig. 4. Activation of caspase-3, -8, and -9. (A) LCL cells were treated with 10 μg/ml of DHMEQ (+) or with DMSO alone (−) for 8 h and fixed on slides. Caspase-3/7, -8, and -9 activities in LCLs after DHMEQ treatment were detected by green fluorochrome-labeled inhibitors of caspases (FLICA)-3/7, -8, and -9 (left panels) and nuclear DNA was stained with Hoechst 33342 (right panels). (B) Effects of DHMEQ on genes regulating apoptosis in LCLs. Quantification of the gene expression by real-time PCR. LCLs were treated with 10 μg/ml of DHMEQ (+) or with DMSO alone (−) for 4 h. The expressions of c-IAP1, Bfl-1, BCL-XL, and c-FLIP were quantified by real-time PCR. The data are means with standard deviation of triplicate experiments. The numbers above the bar graphs indicate the means of each gene expression after DHMEQ treatment. The reduction of the expressions of c-IAP1, Bfl-1, BCL-XL, and c-FLIP was statistically significant.

supershift assays. The results revealed that the NF-κB components consist of p50, p65, and RelB (Fig. 1B).

3.2. DHMEQ induces apoptosis of LCLs

To study the significance of NF-κB activation in the growth of LCLs, we examined the effects of DHMEQ on cell viability. Results of WST-8 assays showed that DHMEQ treatment reduced the cell viability of all four LCLs in a dose- and time-dependent manner (Fig. 2A and B).

NF-κB plays a key role in resistance to apoptosis [18]. Thus, we next examined whether DHMEQ induces apoptosis of LCLs by analyzing Annexin V reactivity and DNA fragmentation. Flow cytometric analysis showed a significant increase in the number of Annexin V-positive cells after DHMEQ treatment (Fig. 3A). Fragmentation of the nuclei of LCLs was clearly demonstrated after DHMEQ treatment by the TUNEL assay (Fig. 3B and C).

3.3. DHMEQ-induced apoptosis involves activation of caspases 3, 8, and 9

To confirm that the induction of apoptosis in LCLs by DHMEQ is caused by activation of the caspase pathway, we first examined activation of caspase-3/7 by immunostaining, using an antibody that recognizes a cleaved form of caspase-3/7. Results clearly showed cleavage of caspase-3/7, confirming that DHMEQ-induced apoptosis is associated with activation of the caspase pathway (Fig. 4A, top). To differentiate the membranous and mitochondrial pathways, we next examined the activation of caspases 8 and 9, which are upstream of caspase-3/7, by immunostaining. DHMEQ-treated LCL cells showed activation of both caspase-8 and caspase-9 (Fig. 4A, middle and bottom).

To understand the molecular mechanisms of apoptosis induction of LCLs after NF-κB inhibition by DHMEQ, we next examined by quantitative RT–PCR the changes in the expression levels of anti-apoptotic genes c-IAP1, Bfl-1, Bcl-XL, and c-FLIP, reportedly under the control of NF-κB, after DHMEQ treatment. The results demonstrated down-regulation of all of these genes (Fig. 4B).

3.4. DHMEQ shows a potent inhibitory effect on the growth of LCL cells in NOG mice

Because results *in vitro* suggested potential efficacy of DHMEQ for the treatment of patients with EBV-associated lymphoproliferative diseases, we next examined whether DHMEQ treatment can suppress the growth of xenografted LCL cells in a NOG mouse model. The gross appearance of resected tumors in mice treated with DHMEQ showed reduction of the tumor mass 1 month after inoculation of LCL cells (Fig. 5A and B). A decrease in the size of tumors in mice treated with DHMEQ was demonstrated when compared with controls 1 month after the injection of LCL cells (Fig. 5C).

3.5. DHMEQ inhibits outgrowth of EBV-infected peripheral blood B-lymphocytes

EBV-infected B lymphocytes under immunocompromised conditions acquire latency III infection, which may lead to proliferation and transformation into lymphoproliferative diseases including lymphomas [2,3]. Previous data link NF-κB activation by LMP-1 to transformation; however, they also indicate that NF-κB activation is not sufficient for transformation and should coordinate with other signals like mitogen-activated protein kinases [19]. Roles of NF-κB activity in EBV-infected lymphocytes for their survival during the early phase of infection are not fully understood. Therefore, to investigate the roles of NF-κB activation on the survival of EBV-infected lymphocytes during the early phase of infection, we examined the effect of NF-κB inhibition by DHMEQ on their survival and the EBV viral load in PBMC infected with EBV. Lymphocytes infected with EBV under immunosuppressive conditions already show constitutive NF-κB activation as well as LMP1 expression. Treatment of these cells with DHMEQ inhibited translocation of NF-κB into the nucleus (Fig. 6A). DHMEQ treatment also eliminated LMP1-expressing lymphocytes from PBMC (Fig. 6B). Finally, DHMEQ treatment prevented the outgrowth of lymphocytes infected

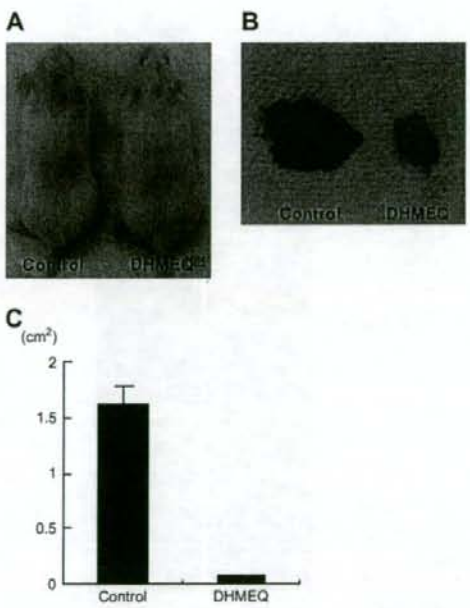

Fig. 5. DHMEQ inhibited the tumor growth of LCL cells *in vivo*. NOG mice were inoculated with LCL cells and administered DHMEQ (12 mg/kg) ($n = 5$) or control medium ($n = 5$) subcutaneously in the post-auricular region three times a week for up to 1 month. (A) Photograph of the backs of mice. (B) Photograph of a tumor at the site of LCL cells inoculation. (C) Subcutaneous tumor volume of mice inoculated with LCL cells and administered DHMEQ or control medium 1 month after inoculation.

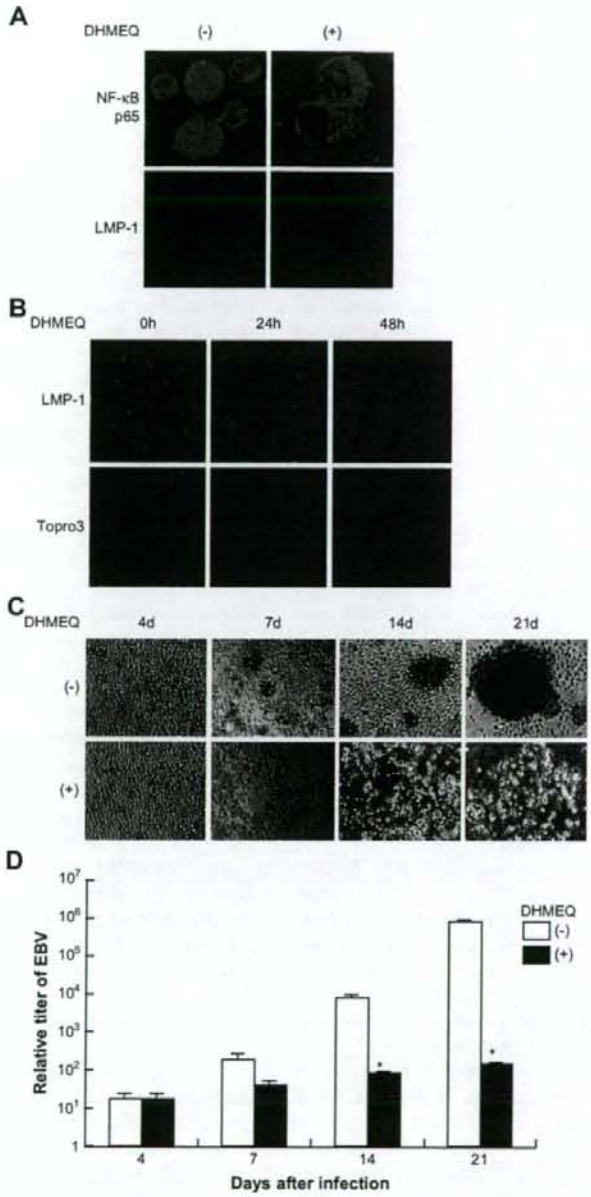

Fig. 6. Effects of DHMEQ on PBMC infected with EBV. 8×10^5/ml of PBMC from a healthy donor infected with EBV using supernatant of B95.8 line were cultured in RPMI 1640 medium supplemented with 10% FBS and 200 ng/ml cyclosporine A. Cells were harvested 4 days and 14 days after infection and served for experiments. (A) Inhibition of NF-κB and expression of LMP1 in lymphocytes. At the point of 4 days after infection, cells were treated with or without 10 μg/ml of DHMEQ for 1 h and immunostained with antibodies for LMP1 and NF-κB p65. DMSO-treated cells served as a control. (B) DHMEQ treatment eliminated LMP1 expressing cells from PBMC. At the point of 14 days after infection, cells were treated with or without 10 μg/ml DHMEQ for the indicated number of hours. Cells stained with anti-LMP1 antibody and topro 3 were observed by confocal microscopy. DMSO-treated cells served as a control. (C, D) Photographs of EBV-infected PBMC and quantification of viral load by real-time PCR. Cells cultured for 4 days were treated with 10 μg/ml of DHMEQ (+) or with DMSO alone (−) thereafter twice a week. Cells were observed by microscopy at the indicated days (C). Cells were harvested on the indicated days and genomic DNA was isolated. The viral load was quantified by real-time PCR as described in Section 2. The data are means and standard deviations of triplicate experiments (D). The asterisks indicate statistical significance.

with EBV and decreased the EBV viral load in PBMC (Fig. 6C and D).

4. Discussion

In the present study, we showed that the NF-κB inhibitor DHMEQ blocked strong and constitutive NF-κB activity, reduced viability, and induced apoptosis in LCLs. Induction of apoptosis by DHMEQ in LCLs is associated with inhibition of NF-κB, which is followed by down-regulation of NF-κB regulated anti-apoptotic genes. These observations, combined with our previous study about the mechanisms of action of DHMEQ [11], indicate that apoptosis induction of LCLs by DHMEQ is mediated by inhibitory effect of DHMEQ against NF-κB. DHMEQ appears to be more specific to NF-κB pathway compared with IκB kinase (IKK) inhibitor, Bay 11-7082 used in the previous studies [20,21], because DHMEQ inhibits downstream of IKK and Bay 11-7082 has been reported to be apparently not specific for NF-κB pathway [22]. Therefore our study provides further evidence for the importance of NF-κB in the survival of LCLs and indicates effectiveness of DHMEQ in the treatment of EBV-infected transformed lymphocytes.

We also showed that DHMEQ inhibits constitutive NF-κB activation in B lymphocytes expressing LMP1, eliminates these cells from PBMC, and inhibits the outgrowth of lymphoblastic cells. The results indicate that B lymphocytes become dependent on NF-κB for proliferation and survival within several days after EBV infection. Although previous data indicate that not only NF-κB but also other signals like mitogen-activated protein kinases are involved in transformation of lymphocytes to LCL cells [19], the results in this study indicates that abrogation of constitutive NF-κB activity appears to be sufficient to prevent transformation of EBV-infected lymphocytes. Previous reports underscored constitutive NF-κB activity as a molecular target in LCL cells [20,21,23]. Our study shows a new insight that constitutive NF-κB activity is a common molecular target in EBV-infected transformed and untransformed lymphocytes.

Recent reports showed that EBV viral load is a useful marker for disease status of lymphoproliferative diseases or lymphomas in patients with immunosuppression [24]. We showed that DHMEQ treatment prevented the increase of EBV viral load in PBMC. The reduction of EBV viral load in PBMC by DHMEQ indicates not only that the elimination of lymphocytes infected by EBV contributes to the reduction, but also that the replication of EBV virus may depend on NF-κB activity. However, previous studies showed that NF-κB activity does not promote replication of EBV virus, but rather inhibits its replication [25]. Therefore, reduction of viral load in lymphocytes infected with EBV treated with DHMEQ appears to be due to the elimination of lymphocytes infected with EBV. Collectively, early detection of the increase of EBV viral load and purging infected cells under transformation by a NF-κB inhibitor may contribute to the preventive intervention against lymphoproliferative diseases in patients with profound immunosuppression.

Our results suggest that the effects of DHMEQ depend on the down-regulation of NF-κB-dependent genes that control apoptosis. Down-regulation of c-FLIP, involved in anti-apoptosis blocking caspase-8, as well as Bfl-1, Bcl-XL and c-IAP, involved in the anti-apoptosis blocking caspase-9, by DHMEQ may result in activation of membranous and mitochondrial pathways, respectively [26]. This implies the possibility that in EBV-infected lymphocytes, the induction of anti-apoptotic genes is counteracting the apoptotic pressure and preventing these cells from undergoing apoptosis.

The mice treated with DHMEQ in 1% DMSO did not show any relevant signs of toxicity such as body weight loss in this experiment. The dose of DHMEQ administered in this experiment was 12 mg/kg three times a week, far less than the LD_{50} of DHMEQ, 180 mg/kg (Naoki Matsumoto, K.U., unpublished observation, July 1999). Results of our in vivo model suggest that DHMEQ may be feasible and less toxic at an effective dose, although the pharmacokinetics has not yet been elucidated. In our NOG mice model, the results indicate that local administration of DHMEQ can prevent primary tumor growth without significant signs of toxicity. Additional experiments, which include intraperitoneal and intravenous administration of DHMEQ, will further confirm efficacy of DHMEQ against LCLs *in vivo*.

Our recent study also indicates that DHMEQ has little effect on the viability of PBMC or purified B cells *in vitro* under almost the same experimental condition as this study [27]. These *in vitro* and *in vivo* results suggest a favorable toxic profile and potent NF-κB inhibitory effect by DHMEQ. Thus, DHMEQ appears to be a candidate for the treatment of EBV-associated lymphoproliferative diseases as well as for their chemoprevention.

In conclusion, our study indicates that the unique NF-κB inhibitor DHMEQ is a potential compound that targets constitutive activation of NF-κB in EBV-infected transformed and untransformed B cells. Because EBV-associated lymphoproliferative diseases are life-threatening and the prognosis of AIDS-associated lymphomas is extremely unfavorable, our results support preventive intervention with a NF-κB inhibitor as a new strategy in patients with immunosuppression.

Acknowledgments

This work was supported in part by Grants-in-Aid for Scientific Research from the Japan Society for Promotion of Science (R.H. and T.W.). This work was also supported by grants from the Japanese Ministries of Education, Culture, Sport Science and Technology and Health, Labour and Welfare, as well as the Human Health Science of Japan (N.Y.).

References

[1] J.I. Cohen, Epstein–Barr virus infection, N. Engl. J. Med 343 (2000) 481–492.
[2] K.F. Macsween, D.H. Crawford, Epstein–Barr virus-recent advances, Lancet Infect. Dis 3 (2003) 131–140.
[3] E. Klein, L.L. Kis, G. Klein, Epstein–Barr virus infection in humans: from harmless to life endangering virus-lymphocyte interactions, Oncogene 26 (2007) 1297–1305.

[4] S. Gottschalk, C.M. Rooney, H.E. Heslop, Post-transplant lymphoproliferative disorders, Annu. Rev. Med 56 (2005) 29–44.
[5] C. Diamond, T.H. Taylor, T. Aboumrad, H. Anton-Culver, Changes in acquired immunodeficiency syndrome-related non-Hodgkin lymphoma in the era of highly active antiretroviral therapy: incidence, presentation, treatment, and survival, Cancer 106 (2006) 128–135.
[6] Y. Hoshida, J.X. Xu, S. Fujita, I. Nakamichi, J. Ikeda, Y. Tomita, S. Nakatsuka, J. Tamaru, A. Iizuka, T. Takeuchi, K. Aozasa, Lymphoproliferative disorders in rheumatoid arthritis: clinicopathological analysis of 76 cases in relation to methotrexate medication, J. Rheumatol 34 (2007) 322–331.
[7] D.C. Guttridge, C. Albanese, J.Y. Reuther, R.G. Pestell, A.S. Baldwin Jr., NF-kappaB controls cell growth and differentiation through transcriptional regulation of cyclin D1, Mol. Cell. Biol. 19 (1999) 5785–5799.
[8] O. Devergne, E. Hatzivassiliou, K.M. Izumi, K.M. Kaye, M.F. Kleijnen, E. Kieff, G. Mosialos, Association of TRAF1, TRAF2, and TRAF3 with an Epstein–Barr virus LMP1 domain important for B-lymphocyte transformation: role in NF-kappaB activation, Mol. Cell. Biol. 16 (1996) 7098–7108.
[9] T.D. Gilmore, Introduction to NF-kappaB: players, pathways, perspectives, Oncogene 25 (2006) 6680–6684.
[10] N. Matsumoto, A. Ariga, S. To-e, H. Nakamura, N. Agata, S. Hirano, J. Inoue, K. Umezawa, Synthesis of NF-kappaB activation inhibitors derived from epoxyquinomicin C, Bioorg. Med. Chem. Lett. 10 (2000) 865–869.
[11] A. Ariga, J. Namekawa, N. Matsumoto, J. Inoue, K. Umezawa, Inhibition of tumor necrosis factor-alpha-induced nuclear translocation and activation of NF-kappa B by dehydroxymethylepoxyquinomicin, J. Biol. Chem. 277 (2002) 24625–24630.
[12] G. Miller, M. Lipman, Comparison of the yield of infectious virus from clones of human and simian lymphoblastoid lines transformed by Epstein–Barr virus, J. Exp. Med 138 (1973) 1398–1412.
[13] N.C. Andrews, D.V. Faller, A rapid micropreparation technique for extraction of DNA-binding proteins from limiting numbers of mammalian cells, Nucleic Acids Res. 19 (1991) 2499.
[14] J. Inoue, L.D. Kerr, L.J. Ransone, E. Bengal, T. Hunter, I.M. Verma, c-rel activates but v-rel suppresses transcription from kappa B sites, Proc. Natl. Acad. Sci. USA 88 (1991) 3715–3719.
[15] M.Z. Dewan, J.N. Uchihara, K. Terashima, M. Honda, T. Sata, M. Ito, N. Fujii, K. Uozumi, K. Tsukasaki, M. Tomonaga, Y. Kubuki, A. Okayama, M. Toi, N. Mori, N. Yamamoto, Efficient intervention of growth and infiltration of primary adult T-cell leukemia cells by an HIV protease inhibitor, ritonavir, Blood 107 (2006) 716–724.
[16] M. Watanabe, M.Z. Dewan, T. Okamura, M. Sasaki, K. Itoh, M. Higashihara, H. Mizoguchi, M. Honda, T. Sata, T. Watanabe, N. Yamamoto, K. Umezawa, R. Horie, A novel NF-kappaB inhibitor DHMEQ selectively targets constitutive NF-kappaB activity and induces apoptosis of multiple myeloma cells in vitro and in vivo, Int. J. Cancer 114 (2005) 32–38.
[17] H. Kimura, M. Morita, Y. Yabuta, K. Kuzushima, K. Kato, S. Kojima, T. Matsuyama, T. Morishima, Quantitative analysis of Epstein–Barr virus load by using a real-time PCR assay, J. Clin. Microbiol. 37 (1999) 132–136.
[18] J. Dutta, Y. Fan, N. Gupta, G. Fan, C. Gelinas, Current insights into the regulation of programmed cell death by NF-kappaB, Oncogene 25 (2006) 6800–6816.
[19] E.D. Cahir McFarland, K.M. Izumi, G. Mosialos, Epstein–Barr virus transformation: involvement of latent membrane protein 1-mediated activation of NF-kappaB, Oncogene 18 (1999) 6959–6964.
[20] E.D. Cahir-McFarland, K. Carter, A. Rosenwald, J.M. Giltnane, S.E. Henrickson, L.M. Staudt, E. Kieff, Role of NF-kappa B in cell survival and transcription of latent membrane protein 1-expressing or Epstein–Barr virus latency III-infected cells, J. Virol 78 (2004) 4108–4119.
[21] S.A. Keller, D. Hernandez-Hopkins, J. Vider, V. Ponomarev, E. Hyjek, E.J. Schattner, E. Cesarman, NF-kappaB is essential for the progression of KSHV- and EBV-infected lymphomas in vivo, Blood 107 (2006) 3295–3302.
[22] J.W. Pierce, R. Schoenleber, G. Jesmok, J. Best, S.A. Moore, T. Collins, M.E. Gerritsen, Novel inhibitors of cytokine-induced IkappaBalpha phosphorylation and endothelial cell adhesion molecule expression show anti-inflammatory effects in vivo, J. Biol. Chem. 272 (1997) 21096–21103.
[23] E.D. Cahir-McFarland, D.M. Davidson, S.L. Schauer, J. Duong, E. Kieff, NF-kappa B inhibition causes spontaneous apoptosis in Epstein–Barr virus-transformed lymphoblastoid cells, Proc. Natl. Acad. Sci. USA 97 (2000) 6055–6060.
[24] S.M. Aalto, E. Juvonen, J. Tarkkanen, L. Volin, T. Ruutu, P.S. Mattila, H. Piiparinen, S. Knuutila, K. Hedman, Lymphoproliferative disease after allogeneic stem cell transplantation–pre-emptive diagnosis by quantification of Epstein–Barr virus DNA in serum, J. Clin. Virol 28 (2003) 275–283.
[25] H.J. Brown, M.J. Song, H. Deng, T.T. Wu, G. Cheng, R. Sun, NF-kappaB inhibits gammaherpesvirus lytic replication, J. Virol 77 (2003) 8532–8540.
[26] J.M. Adams, Ways of dying: multiple pathways to apoptosis, In: Genes Dev, 17 (2003) 2481–2495.
[27] R. Horie, M. Watanabe, T. Okamura, M. Taira, M. Shoda, T. Motoji, A. Utsunomiya, T. Watanabe, M. Higashihara, K. Umezawa, DHMEQ, a new NF-kappaB inhibitor, induces apoptosis and enhances fludarabine effects on chronic lymphocytic leukemia cells, Leukemia 20 (2006) 800–806.

ELSEVIER

INSTITUT PASTEUR

Microbes and Infection 10 (2008) 471–480

www.elsevier.com/locate/micinf

Original article

Statin-induced inhibition of HIV-1 release from latently infected U1 cells reveals a critical role for protein prenylation in HIV-1 replication

Tohti Amet [a], Mizuho Nonaka [a], Md. Zahidunnabi Dewan [a,b], Yasunori Saitoh [a], Xiaohua Qi [a,b], Shizuko Ichinose [c], Naoki Yamamoto [a,b], Shoji Yamaoka [a,*]

[a] *Department of Molecular Virology, Graduate School of Medicine, Tokyo Medical and Dental University, 1-5-45 Yushima, Bunkyo-ku, Tokyo 113-8510, Japan*

[b] *AIDS Research Center, National Institute of Infectious Diseases, Shinjuku-ku, Tokyo 162-8640, Japan*

[c] *Instrumental Analysis Research Center, Tokyo Medical and Dental University, 1-5-45 Yushima, Bunkyo-ku, Tokyo 113-8510, Japan*

Received 20 November 2007; accepted 14 January 2008
Available online 20 January 2008

Abstract

Latent infection of human immunodeficiency virus type 1 (HIV-1) represents a major hurdle in the treatment of acquired immunodeficiency syndrome (AIDS) patients. Statins were recently reported to suppress acute HIV-1 infection and reduce infectious virion production, but the precise mechanism of inhibition has remained elusive. Here we demonstrate that lypophilic statins suppress HIV-1 virion release from tumor necrosis factor alpha-stimulated latently infected U1 cells through inhibition of protein geranylgeranylation, but not by cholesterol depletion. Indeed, this suppression was reversed by the addition of geranylgeranylpyrophosphate, and a geranylgeranyltransferase-1 inhibitor reduced HIV-1 production. Notably, silencing of the endogenous Rab11a GTPase expression in U1 cells by RNA interference destabilized Gag and reduced virion production both in vitro and in NOD/SCID/γc^{null} mice. Our findings thus suggest that small GTPase proteins play an important role in HIV-1 replication, and therefore could be attractive molecular targets for anti-HIV-1 therapy.

Keywords: Statins; Prenylation; HIV-1; Rab11a; Small GTPases

1. Introduction

Infection with human immunodeficiency virus type 1 (HIV-1), the causative agent of acquired immunodeficiency syndrome (AIDS), is characterized clinically by a long asymptomatic period of latency preceding the development of AIDS. Even during this period of latency, the virus is continuously replicating and causing *de novo* infection. Recent studies using combination anti-retroviral therapy have revealed a population of latently infected cells that are refractory to antiviral therapy, which is believed to be a leading cause of the persistence of infection [1]. Although patients treated successfully with the highly active anti-retroviral therapy (HAART) achieved undetectable levels of virus load, viremia recurred in almost every patient when the drug therapy was stopped, because latent virus in reservoir cells is not susceptible to this anti-retroviral therapy or host immune responses [2,3]. Thus, HIV-1 infection remains incurable and new therapeutic approaches need to be developed.

Recent studies have suggested that lypophilic statins have direct anti-HIV effects. del Real et al. showed that lovastatin reduced acute infection by HIV-1 NL4-3.Luc.R.E. pseudotyped with HIV-R5 or X4 envelopes, but not that by the virus pseudotyped with the vesicular stomatitis virus glycoprotein (VSV-G) envelope. Lovastatin treatment of HEK 293T producer cells also reduced HIV-1-X4-enveloped infectious virus production, but not that of VSV-G-pseudotyped virus. The

* Corresponding author. Tel.: +81 3 5803 5181; fax: +81 3 5803 0124.
E-mail address: shojmmb@tmd.ac.jp (S. Yamaoka).

1286-4579/$ - see front matter © 2008 Elsevier Masson SAS. All rights reserved.
doi:10.1016/j.micinf.2008.01.009

proposed mechanism was that statins targeted Rho GTPases and affected the actin cytoskeleton re-arrangement necessary for virus entry or budding [4,5]. It was also reported that statins suppressed virion-associated intercellular cell adhesion molecule 1—leukocyte function antigen 1 interactions that are required for viral entry [6]. Audoly et al., using inhibitory toxins, proposed that small GTP-binding proteins are involved in the assembly of HIV-1 Gag in their acute infection model [7]. Quite recently, Nabatov et al. reported that statins disrupt CCR5 and RANTES expression levels in CD4+ T lymphocytes in vitro and preferentially decrease infection of R5 versus X4 HIV-1 [8]. However, the effect of statins in chronically HIV-1-infected cells and its precise mechanism remain to be uncovered.

Statins, which are used to treat hypercholesterolemia, inhibit 3-hydroxy-3-methylglutaryl coenzyme A (HMG-CoA) reductase, the rate-limiting enzyme in cholesterol biosynthesis in the liver catalyzing the conversion of HMG-CoA to mevalonic acid [9,10]. In addition to inhibiting cholesterol synthesis, statins also block the synthesis of isoprenoid intermediates such as farnesylpyrophosphate (FPP) and geranylgeranylpyrophosphate (GGpp). Both FPP and GGpp serve as important lipid attachments for the post-translational modification of variety of proteins, including heterotrimeric G proteins and small GTP-binding proteins such as the Ras, Rho, Rap, and Rab GTPase family proteins [11,12]. This modification, called protein prenylation, is a common mechanism for membrane association of approximately 0.5% of all intracellular proteins. Prenylation consists of the covalent attachment, via thioether linkage, of a C15 (farnesyl) or C20 (geranylgeranyl) isoprenoid group to a C-terminal cysteine residue in the context of a 'prenylation motif'. Farnesyl and geranylgeranyl moieties can bind covalently to several low molecular weight GTPase proteins, and this binding is catalyzed by three prenyltransferases: farnesyltransferase (FTase), geranylgeranyltransferase-1 (GGTase-I) or geranylgeranyltransferase-2 (GGTase-2, also called Rab GGTase). Thus, inhibition of the mevalonate pathway or geranylgeranyltransferases leads to impairment of protein prenylation.

Protein prenylation is critical for intracellular localization and function of small GTPase proteins. In general, modification with FPP is necessary for proper localization of Ras family proteins, whereas GGpp is required for Rho, Rab, and Rap family proteins. Among them, Rab GTPase proteins form the largest family within the Ras-like GTPase superfamily [13,14]. More than 50 Rab proteins have been identified in mammalian cells. Each Rab is believed to be localized to a specific subcellular compartment, reflecting the complexity and variety of trafficking events found in mammalian cells. Rab proteins, unlike other small GTPases, exhibit a variety of prenylation motifs at their C-termini, containing either one or more frequently, two cysteine residues, both of which are modified by geranylgeranyl groups [15]. It was recently reported that siRNA-mediated silencing of Rab9 expression in JC53 HeLa-derived indicator cells inhibited HIV replication, as did silencing expression of other genes that facilitate the late-endosome-to-*trans*-Golgi vesicular transport [16]. Interestingly, acute HIV-1 replication in JC53 cells was also affected, although less profoundly, by silencing expression of Rab11a. It has been well documented that Rab11a is mainly located on pericentriolar recycling endosomes and plays a key role in regulating vesicle trafficking through recycling endosomes to the plasma membrane as well as in exocytosis [17,18].

Here we investigated the effect of statins on virus production in chronically HIV-1-infected promonocytic U1 cells, and showed a critical role for protein prenylation in the late phase of HIV-1 replication.

2. Materials and methods

2.1. Reagents and cells

Simvastatin and lovastatin were purchased from LKT Laboratories, Inc. (MN, USA), and activated by dissolving in ethanol and treatment with 0.1 M NaOH. The pH was then adjusted to 7.0 with HCl. GGTI-298 and FTI-277 were purchased from Calbiochem (Darmstadt, Germany). Anti-Rab11a monoclonal antibody was purchased from BD transduction laboratories (Japan). The serum derived from an HIV-1-infected patient was described previously [19]. Anti-mouse IgG (H&L), anti-human rabbit HRP-linked antibody was obtained from American Qualex manufactures (CA, USA). DMRIE-C reagent for transfection was purchased from Invitrogen (CA, USA). All other reagents including anti-tubulin (T-9026) monoclonal antibody, squalene, GGpp, cycloheximide, TNF-α and phorbol-12-myristate-13 acetate (PMA) were purchased from Sigma (MO, USA). U1 and HEK 293T cells were grown in RPMI 1640 and DMEM, respectively, supplemented with 10% heat-inactivated fetal bovine serum, 100 U/ml of penicillin and streptomycin at 37 °C.

2.2. Treatment and stimulation of cells

Cells were treated with or without simvastatin or lovastatin for 2 days and equivalent numbers of viable cells were stimulated with TNF-α or PMA for additional 2 days in the presence or absence of statins, and then intracellular and extracellular Gag (p24 and p55) antigen was quantified. More than 80% of cells were found viable after treatment with 1 μM of simvastatin, and we normalized the levels of Gag protein (p24 and p55) based on the number of viable cells in each sample. The amount of Gag per viable cell was calculated by dividing the Gag value with the number of viable cells. In some of the experiments, GGpp (1 μM), squalene (50 μg/ml) or GGTI-298 (1 μM) was added during the entire course of the experiment.

2.3. HIV-1 Gag quantification

Culture supernatant was collected after centrifugation and subjected to quantification of the HIV-1 Gag (p55 and p24) antigen by automated enzyme-linked immunosorbent assay (ELISA) (Fuji Rebio Inc., Tokyo, Japan). Cell pellets were

washed three times with PBS, re-suspended with the p24 lysis buffer (0.5% Triton X-100 in PBS), put on ice for 30 min, and then the Gag antigen was quantified by using auto-ELISA system. The amount of Gag was normalized by dividing the Gag value with the number of viable cells. The relative amounts of Gag were expressed as percentages of that for cells simply stimulated with TNF-α or PMA (arbitrarily set at 100%). The ratio of Gag amount in culture supernatant to that in cells was calculated by dividing the normalized Gag amount in supernatant with that in cell lysate.

2.4. Western blotting

Cells were lysed in a lysis buffer (20 mM Tris–HCl [pH 8.0], 150 mM NaCl, 1% Triton X-100, 10% glycerol, 0.5 mM dithiothreitol, 0.5 mM phenylmethanesulphonylfluoride (PMSF), 0.1% aprotinin, and 0.1% leupeptin) for preparation of whole-cell extracts. Thirty micrograms aliquots of protein, determined by the Bradford assay, were resolved by SDS–PAGE and detected by standard immunoblotting procedures using the specific primary antibodies.

2.5. Transmission electron microscopy

Cells were fixed with 2.5% glutaraldehyde in PBS for 2 h, washed and fixed overnight at 4 °C in the same buffer and post-fixed with 1% OsO_4 buffered with PBS for 2 h. The cells were then dehydrated in a graded series of ethanol and embedded in Epon 812. Ultrathin (90 nm) sections were cut on an ultracut S microtome (Reichert, Vienna, Austria), double-stained with uranyl acetate and lead citrate, and then examined by transmission electron microscopy (H-7100, Hitachi, Hitachinaka, Japan).

2.6. Lentivirus vectors

Annealed oligonucleotides containing the targeting *rab11a* (5′-GAGCGATATCGAGCTATAA-3′) or *Renilla luciferase* (5′-GTAGCGCGGTGTATTATAC-3′) sequence were first inserted immediately downstream of the H1 promoter of the pSuperRetro vector (Oligoengine), generating pSR-Rab11a-i and pSR-Ctrl-i, respectively. The shRNA expression cassettes were then transferred to a newly constructed lentivirus vector, pCS-puro-PRE, carrying a puromycin resistance gene expressed under the control of the phosphoglycerate kinase (PGK) promoter. Construction details for pCS-puro-PRE will be described elsewhere (Saitoh et al., unpublished). EcoRI–XhoI fragments containing the H1 promoter and targeting sequence from pSR-Rab11a-i or pSR-Ctrl-i were inserted between the EcoRI and XhoI sites of pCS-puro-PRE, generating pCS-puro-Rab11a-i and pCS-puro-Ctrl-i, respectively.

2.7. Transfection and infection

The VSV-G-pseudotyped lentivirus was produced by co-transfection of HEK 293T cells with pCS-puro-Rab11a-i or pCS-puro-Ctrl-i, pHCMV-VSV-G encoding the vesicular stomatitis virus glycoprotein (VSV-G) and a packaging construct pCMVΔR8.2 (a kind gift from ISY Chen, USA), using FuGENE 6 (Roche Diagnostics, IN, USA) according to the manufacturer's instructions. Culture supernatants of 293T cells were collected 48 h post-transfection, filtered through 0.20-μm pore-size filters, supplemented with polybrene (10 μg/ml), and used immediately for infection of U1 cells. Infected cells were selected in the presence of 3 μg/ml of puromycin.

2.8. Animal experiments

NOD/SCID/γc^{null} (NOG) mice were obtained from the Central Institute for Experimental Animals (Kawasaki, Japan). All mice were maintained under specific pathogen-free conditions in the animal center of Tokyo Medical and Dental University (Tokyo, Japan). The Ethical Review Committee of the Institute approved the experimental protocol. NOG mice were inoculated intraperitoneally with approximately 2.5×10^6 Rab11a-depleted or control U1 cells per mouse as described previously [20]. Blood and ascites were examined for HIV-1 p24 amount 2 weeks after cell inoculation.

3. Results

3.1. Statins suppressed HIV-1 release from U1 cells

We used U1 cells that do not constitutively produce or release HIV-1 virions to the culture supernatant. U1 cells are derived from U937 promonocytic cells that survived the cytopathic effect associated with the acute infection by HIV-1 LAI/IIIB. U1 cells contain two integrated copies of proviral HIV-1 DNA and are characterized by low constitutive levels of virus expression that can be up-regulated by several cytokines and phorbol esters. Upon stimulation of U1 cells with PMA or with cytokines such as TNF-α, a dramatic increase in HIV-1 gene expression and robust virion release can be induced. Virions were shown to be released from U1 cells in a manner similar to that for cells of monocytic lineage [21,22]. U1 cells were treated with or without simvastatin for 48 h and then stimulated with TNF-α. We found that treatment of U1 cells with 1 μM of simvastatin, which is within the clinically relevant range, suppressed TNF-α-induced release of p24 to culture supernatant (Fig. 1A). Conversely, intracellular Gag protein (including both p55 and its processed form p24) was increased after the treatment with simvastatin and TNF-α. As a result, the ratio of Gag in culture supernatant to Gag in cell lysate was reduced (Fig. 1B). The release of p24 from cells treated with simvastatin and PMA (Fig. 1A,B) was not profoundly suppressed, but this treatment increased intracellular level of Gag. Essentially similar results were obtained with another lipophilic statin lovastatin (Fig. 1C,D), but not with hydrophilic paravastatin (data not shown), suggesting that lypophilic statins, such as simvastatin and lovastatin, successfully entered cultured cells and worked as HMG-CoA reductase inhibitors.

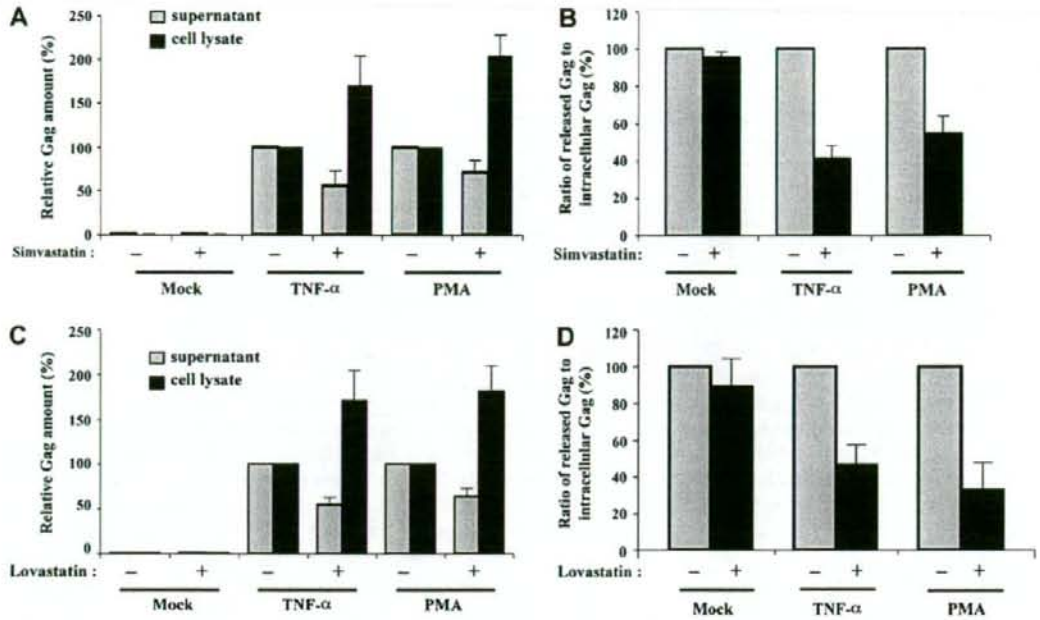

Fig. 1. Statins reduced virus release and increased intracellular Gag in U1 cells. U1 cells were treated or not with simvastatin (A) or lovastatin (C) for 2 days, followed by stimulation with TNF-α (1 ng/ml) or PMA (1 ng/ml) for additional 2 days in the continued presence or absence of simvastatin or lovastatin. Gag (p24 and p55) in culture supernatants (gray bars) and in cell lysates (filled bars) were then quantified. (A) and (C) The relative amounts of Gag in statin-treated (+) cultures are shown in percentage of that of cells (−) stimulated with TNF-α or PMA alone (arbitrarily set at 100%). (B) and (D) Ratios of released Gag to intracellular Gag for statin-treated cells are shown in percentage of the ratio obtained for cells simply stimulated with TNF-α or PMA (arbitrarily set at 100%). Results shown are mean ± SD values of three independent experiments.

3.2. Geranylgeranylation is required for HIV-1 replication in U1 cells

A previous report showed that treatment of 293T cells with lovastatin reduced production of wild type, but not VSV-G-pseudotyped HIV-1, and that this inhibition was reversed by the addition of GGpp [4]. To examine if the reduced p24 release from U1 cells treated with simvastatin resulted from impaired production of geranylgeranyl, we treated U1 cells with simvastatin and TNF-α in the presence of 1 μM GGpp (Fig. 2A). No cytotoxicity was observed after the treatment with GGpp. Addition of GGpp restored the p24 release to the level for control cells stimulated with TNF-α. In contrast, the amount of Gag in cells treated with simvastatin and TNF-α in the presence of GGpp remained higher than that in cells treated with simvastatin and TNF-α. Squalene, one of the metabolites in the cholesterol biosynthesis from FPP, did not interfere with simvastatin-induced inhibition of virion release or intracellular Gag protein accumulation (Fig. 2B). To further investigate the importance of protein prenylation in HIV-1 replication in U1 cells, we tested if geranylgeranyltransferase-1 inhibitor (GGTI) could inhibit virus replication. GGTI was not toxic to U1 cells at 1 μM, whereas farnesyltransferase inhibitor (FTI) was too toxic to be tested in U1 cells (data not shown). GGTI reduced both p24 release and intracellular Gag in TNF-α-stimulated U1 cells (Fig. 2C), suggesting that geranylgeranylation of small GTPase proteins plays a critical role in HIV-1 production.

3.3. Simvastatin enhances intracellular Gag accumulation in U1 cells

We next examined how simvastatin modifies expression of intracellular HIV-1 Gag-related proteins, p55 and its processed form p24. Immunoblotting with anti-HIV-1 Gag antiserum that detected both p55 and p24 revealed that p24 was increased in the presence of simvastatin, while the amount of p55 remained almost unchanged (Fig. 3A). Since the results shown in Fig. 2A suggested the importance of geranylgeranylation, we examined the prenylation status of Rab11a, one of the Rab family small GTPases known to be involved in trafficking of recycling endosomes and exocytosis. As shown in Fig. 3A, treatment with 1 μM simvastatin resulted in almost complete upward shifting of the Rab11a band, indicating accumulation of the non-prenylated form of Rab11a. Besides, GGpp counteracted the simvastatin effect on the prenylation of Rab11a (Fig. 3B). This suggests that simvastatin inhibited the biosynthesis of geranylgeranyl, leading to impaired prenylation of small GTPases involved in intracellular vesicle trafficking. To further gain insight into the effects of simvastatin on HIV-1 replication, we performed transmission electron microscopic (TEM) analysis. Many virus particles were found to be

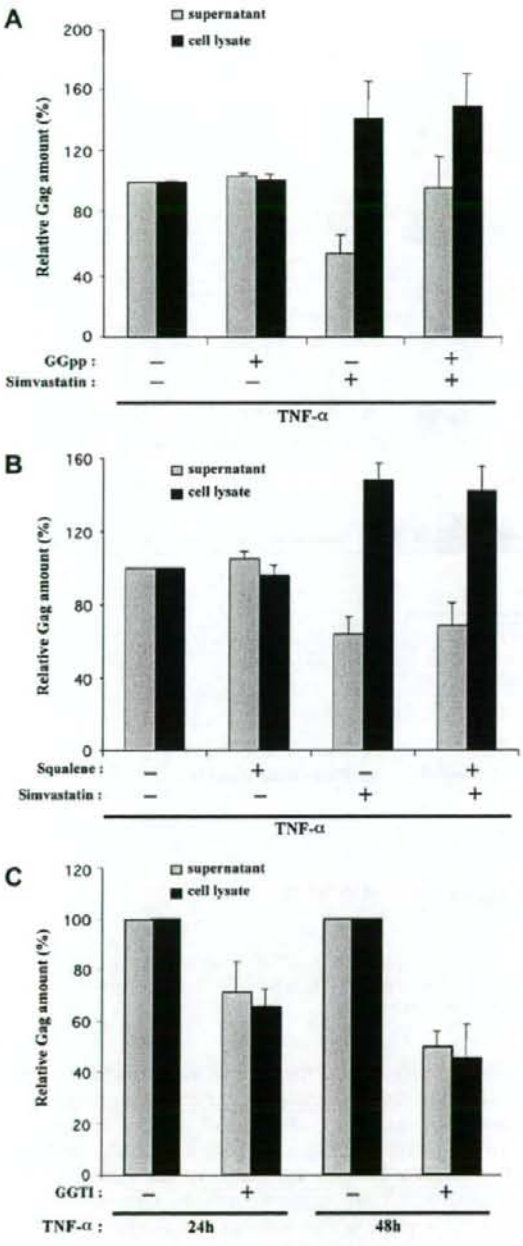

Fig. 2. GGpp restored simvastatin-inhibited virion release, and GGTI suppressed HIV-1 Gag production in U1 cells. U1 cells were cultured for 2 days in the presence (+) or absence (−) of simvastatin, GGpp (A), squalene (B), and GGTI (C). Cells were then stimulated with TNF-α (1 ng/ml) for additional 1 or 2 days, and Gag in supernatants (hatched bars) and cell lysates (filled bars) was quantified. The relative amounts of Gag are shown in percentage of that of cells simply stimulated with TNF-α (arbitrarily set at 100%). Data shown are mean ± SD values of three independent experiments.

released from TNF-α-stimulated U1 cells in the mature form (Fig. 4A,B), but only a few from simvastatin- and TNF-α-treated U1 cells. In contrast, many mature virus particles could be seen in intracellular vesicles of U1 cells treated with simvastatin and TNF-α, whereas it was difficult to find mature virions in vesicles of U1 cells treated with TNF-α alone (Fig. 4C,D). These results suggested impaired release or intracellular trafficking of virions.

3.4. Rab11a mediates HIV-1 replication in U1 cells

In order to further investigate the role of Rab11a in HIV-1 replication in U1 cells, we suppressed the expression of endogenous Rab11a by RNA interference. Immunoblotting analyses (Fig. 5A) demonstrated that the level of Rab11a expression was reduced by ~80–90% in cells expressing Rab11a-specific shRNA (Rab11a-i) compared to cells expressing control shRNA (Ctrl-i). While Rab11a depletion did not affect the growth of U1 cells (data not shown), it reduced the release of p24 as well as intracellular Gag expression induced by TNF-α (Fig. 5B). Immunoblotting analyses revealed that both p24 Gag and p55 Gag are decreased in Rab11a-depleted cells compared to control cells (Fig. 5C). These findings indicate that HIV-1 requires Rab11a for its efficient replication in U1 cells. We next examined if Rab11a depletion affects the stability of Gag, using a protein synthesis inhibitor cycloheximide. As shown in Fig. 5C, the levels of p55 Gag and p24 Gag in Rab11a-depleted cells were generally lower than those in control cells. Importantly, while the expression of p55 Gag remained almost unchanged up to 12 h after CHX treatment in control cells, p55 Gag in Rab11a-depleted cells rapidly decreased with a half-life of ~6 h (Fig. 5D,E). The expression of p24 Gag in Rab11a-depleted cells was lost even more rapidly following cycloheximide treatment, while p24 Gag was only marginally reduced in control cells. These results indicate that Rab11a depletion reduced the stability of Gag, which led to inefficient viral replication in U1 cells.

3.5. Rab11a depletion affects HIV-1 replication in NOG mice

The significant suppression by Rab11a depletion of TNF-α-induced HIV-1 replication in cultured U1 cells prompted us to examine whether depletion of Rab11a in U1 cells can also suppress virus replication in NOG mice. We inoculated Rab11a-depleted or control U1 cells in the peritoneal cavity of immune-deficient NOG mice. Blood and ascites were recovered 2 weeks after inoculation, and then the Gag amounts were determined. Knockdown of Rab11a expression in U1 cells did not apparently influence the growth of cells in mice, but efficiently suppressed HIV-1 replication *in vivo* as revealed by Gag amounts in both serum and ascites (Fig. 6A,B).

4. Discussion

The inhibition of HIV-1 replication by statins was previously reported in acute HIV-1 infection models, and three

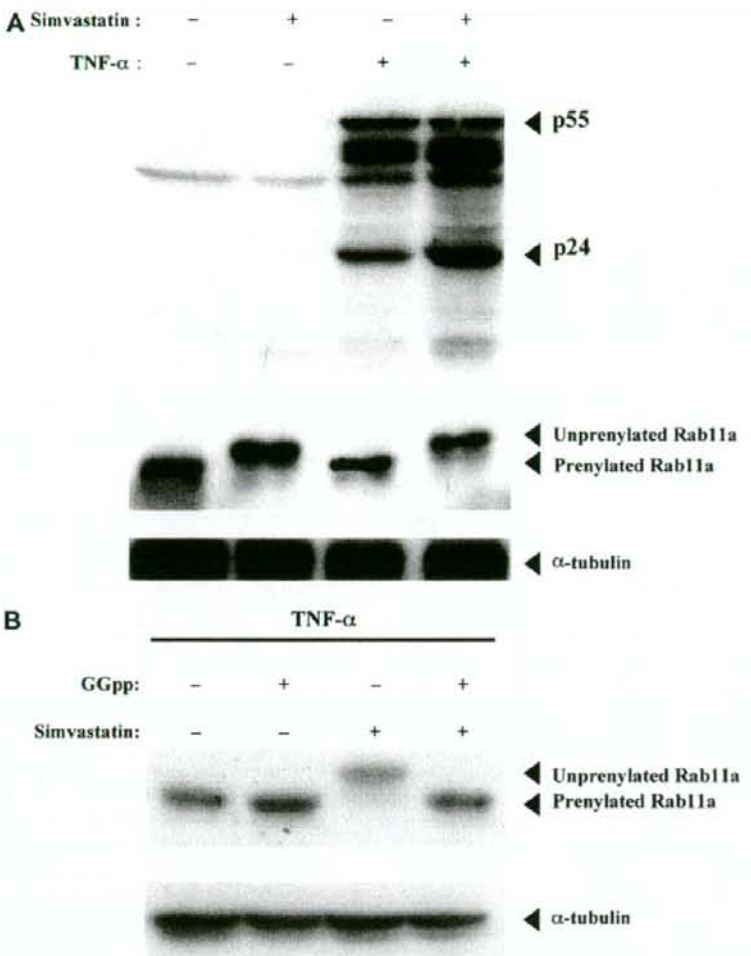

Fig. 3. Simvastatin increased p24 and ablated prenylation of Rab11a in U1 cells. U1 cells were incubated for 2 days with or without simvastatin (A) or GGpp (B), and then stimulated with TNF-α in the continued presence or absence of simvastatin or GGpp for additional 2 days. Whole-cell lysates were prepared and subjected to immunoblotting with serum derived from an HIV-1-infected patient or antibodies to Rab11a or α-tubulin.

different mechanisms were proposed. First, inhibition of HMG-CoA reductase activity resulted in impaired synthesis of GGpp required for prenylation of a small GTPase protein Rho [4]. Second, direct binding of statins to lymphocyte-function-associated antigen 1 (LFA-1) diminished HIV-1 attachment to target cells by preventing the interaction between virion-associated host intercellular adhesion molecule 1 and its natural cell surface ligand LFA-1 [6]. Third, statins disrupted CCR5 and RANTES expression [8]. In this report, we showed statin-induced increase in intracellular Gag and decrease in virus release from chronically HIV-1 infected cells, and defined diminished geranylgeranylation as a principal mechanism of statin-induced inhibition of virus release. The inhibition was associated with nearly a complete loss of prenylation of a small GTPase protein Rab11a, which facilitates vesicle trafficking to the plasma membrane from both the *trans*-Golgi network and recycling endosomes. Indeed, RNA interference-mediated silencing of Rab11a expression also led to a marked reduction in both intracellular and secreted Gag protein. These observations are not limited to TNF-α-induced HIV-1 production in vitro, because the silencing of Rab11a expression also reduced p24 release from U1 cells inoculated in immune-deficient mice.

The effects of simvastatin on HIV-1 replication in U1 cells, increase in intracellular Gag and decrease in virus release, cannot solely be explained by the loss of functional small GTPases involved in vesicle trafficking, because supplementing GGpp in the presence of simvastatin, indeed, restored virus release, but did not normalize the level of intracellular Gag. The increase in intracellular Gag by simvastatin treatment

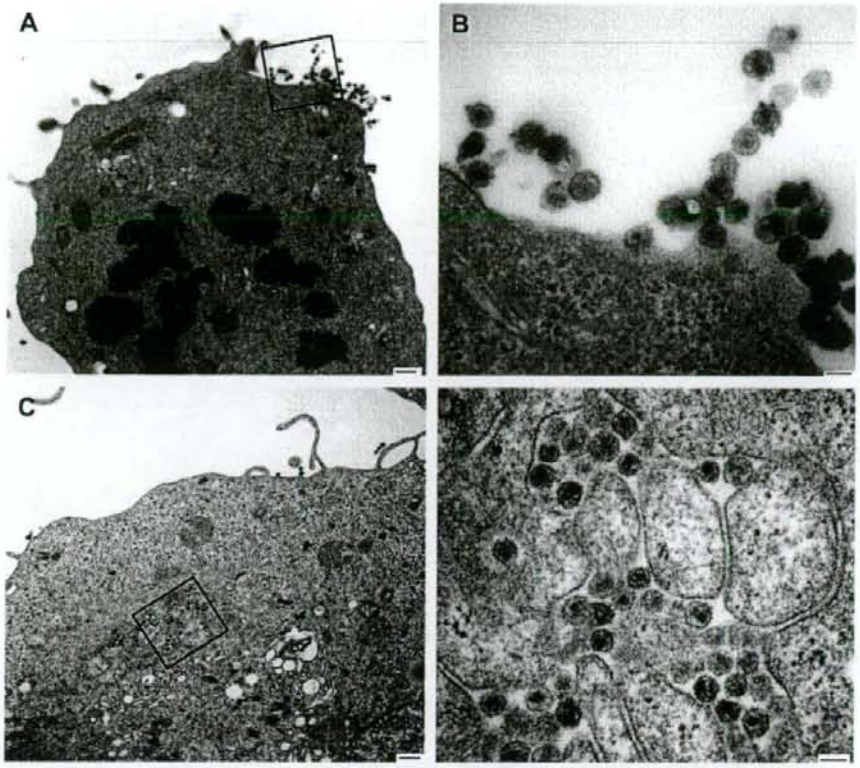

Fig. 4. Transmission electron microscopic (TEM) images of U1 cells. (A) TNF-α-stimulated U1 cell. Many HIV-1 particles are visible at the cell surface. Bar indicates 500 nm (10,000×). (B) Higher magnification of the area indicated by the square in (A). The cone-shaped core structure is evident. Bar indicates 100 nm (60,000×). (C) U1 cell treated with simvastatin and TNF-α. Large vesicles near the Golgi zone contain maturated HIV-1 particles. Bar indicates 500 nm (10,000×). (D) Higher magnification of the area indicated by the square in (C). Bar indicates 100 nm (60,000×).

might simply be a result of accumulation of virions due to impaired virion release, but the results of more specified inhibition by GGTI or gene silencing indicate that loss of prenylation or depletion of Rab11a GTPase reduces both intracellular and extracellular Gag. Thus, simvastatin appears to have yet unknown actions to increase intracellular p24 in U1 cells. In this regard, simvastatin may potentially enhance production of Gag as lovastatin was previously reported to augment HIV-1 LTR-directed transcription in Jurkat cells [4]. The inhibition of virus release by simvastatin would, therefore, be due to loss of prenylation of a yet unidentified protein.

Recent reports support a model of intracellular Gag trafficking common to a variety of cell types in which Gag localizes initially to perinuclear clusters, and then to late endosomes and MVBs and/or MVB-like compartments [23,24]. Both in macrophages and dendritic cells, HIV-1 Gag can be detected in CD63-positive late endosomes and viral exit proceeds through TSG101-dependent budding into the lumen of late endosomes to form multivesicular bodies, followed by the export of viral particles as exosomes [25–28]. However, the transport mechanism of endosomal compartments or MVBs to the cell surface during the course of viral maturation and budding remains to be fully elucidated. Small GTPase proteins have been reported to be involved in vesicle trafficking and actin polymerization. It should be noted that Rab11a is mainly located on pericentriolar recycling endosomes and regulates vesicle trafficking through recycling endosomes to the plasma membrane as well as release of exosomes [29]. In the present report, depletion of Rab11a resulted in an obvious destabilization of Gag p55 and p24, suggesting that Gag failed to traffic through the endosomal compartments or MVBs and could be directed to lysosomal degradation.

Since lipophylic statins cannot be used for HIV-1 infected patients due to its pharmacokinetic interaction with protease inhibitors, inhibiting prenylation of small GTPases involved in Gag trafficking by GGTIs could represent an alternative strategy for effective anti-HIV-1 therapy. GGTI used in this study was previously reported to arrest human tumor cells in G0/G1 and induces $p21^{WAF1/CIP1/SDI1}$ expression in a p53-independent manner and was considered potentially useful in cancer therapy [30]. Perhaps, specific inhibition of individual GTPases involved in HIV-1 replication such as Rab11a would